Universidade Federal de Itajubá - UNIFEI
Programa de Pós Graduação em Física - PGF

Dissertação de Mestrado

Optical Analogue Models for Black Holes and Wormholes

Diego Renan da Silva

Itajubá - MG
30 de Julho de 2020

Universidade Federal de Itajubá - UNIFEI
Programa de Pós Graduação em Física - PGF

Dissertação de Mestrado

Optical Analogue Models for Black Holes and Wormholes

Aluno: Diego Renan da Silva
Orientador: Renato Klippert Barcellos

Dissertação de Mestrado apresentada ao Programa de Pós-Graduação em Física da Universidade Federal de Itajubá (área de concentração: Física), como parte dos requisitos necessários para a obtenção do Título de Mestre em Ciências em Física.

Itajubá - MG
30 de Julho de 2020

Dedicatória

Aos meus pais Francisco e Ronilda,
por sempre estarem comigo em todos os momentos.

Acknowledgements

I thank God for still another achievement in my life.

I thank my father Francisco and my mother Ronilda, for all their support and motivation throughout my academic career.

I thank my beloved girlfriend Gislaine, for all the support and companionship over this time.

I thank all my family members for being together with me along this trajectory, and in particular, my dear grandmother Joselina, for the daily company we offer to each other.

I thank my advisor, Renato Klippert, for all the advices, patience and help during this period. I learned a lot during these 2 years that we worked together, not only physics matters, but also about life!

I thank to my colleagues and friends from this master course who were part of this trajectory, either in the disciplines or in the simple collaborations with the work.

I thank to the professors who were part of all my academic growth.

I thank to CAPES for the financial support to carry out this research work.

"Ainda que eu andasse pelo vale da sombra da morte, não temeria mal algum, porque tu estás comigo; a tua vara e o teu cajado me consolam."

(Salmos 23:4)

Abstract

This work aims to present and discuss the optical analogue models used to study gravitational systems using condensed matter systems. The whole mathematical theory behind the construction of an analogue optical model and the explicit presentation of two analogue models are provided: Schwarzschild black hole and Morris-Thorne wormhole. A parametrization of such models is proposed in order to unify them through a free real parameter β that generates a family of new models, and open the possibility that some of theses new models could actually be analogue models.

Keywords: Optical Analogue Model, black holes, wormholes.

Resumo

Este trabalho tem como objetivo apresentar e discutir os modelos análogos ópticos utilizados para estudar sistemas gravitacionais por meio de sistemas de matéria condensada. Toda teoria matemática por trás da construção de um modelo análogo óptico é apresentada, juntamente com dois modelos: o buraco negro de Schwarzschild e o buraco de minhoca de Morris-Thorne. Propõe-se uma parametrização de tais modelos de modo a unificá-los por meio de um parâmetro real livre β que gera uma família de novos modelos e abre possibilidade de que alguns desses novos modelos venham a ser modelos análogos.

Palavras-chaves: Modelos análogos ópticos, buracos negros, buracos de minhoca.

List of Figures

Contents

Chapter 1

Introduction

The evolution of physics usually requires the combination of theoretical and experimental results. However, the experimental study is not always easy to perform, as is the case of the study of gravitational systems (like black holes and wormholes), due to measurement impossibilities. Fortunately, there is a tool that helps in these situations, known as analogue models: material media inside which the propagation of signals of some type can be described as curve lines which are null geodesics of some effective geometry.

The analogue models are tools to study particular physical systems with the help of some other particular physical system which displays similarity in the propagation of signals. Thus, there is the possibility of studying hardly accessible gravitational systems, such as black holes and wormholes, by means of systems one can produce in the laboratory. The first time this was achieved was in the work presented by Gordon [1], who proposed to describe the refraction index of isotropic medium at rest as an effective change in the metric properties of the flat (Minkowski) spacetime.

After Gordon's work, several analogue models for acoustic, hydrodynamic and optical systems were developed [2–4]. The theme achieved great relevance in 1981 with Unruh's proposal [5] of a theoretical hydrodynamic system which was shown to mimic Hawking radiation of black holes. This issue was recently examined in laboratory by means of analogue models [6, 7]. Therefore, analogue models are a great tool for the study of gravitational systems through condensed matter systems, and thus have a wide range of applications [4].

The present work aims to provide a measurement of the (quantitative) difference between a black hole and a wormhole, in order to establish the frontier between these two models. An interpolation (and extrapolation) is given of the analogue models of two paradigmatic models of general relativity: the Schwarzschild black hole and the Morris-Thorne wormhole. In Chapter 2, both these models are presented, with the metric that describes each structure. That chapter also deals with the theory of analogue models; that is, it includes all the mathematical apparatus necessary to understand the optical analogue models which are discussed in this work. The obtention of an effective metric of the problem is presented in details, which is then used for the comparison with the gravitational metrics. This effective metric is obtained by using the Hadamard method of dealing with abruptly varying fields, a technique discussed in details in Section 2.2.2.

In Chapter 3, the analogue models for the two geometries discussed in Chapter 2 are presented. For each model, the corresponding analogue quantities are determined, namely, the volumetric density of electric charge, the electric permittivity, the electric displacement vector field and the electric vector field. These quantities, taken altogether, completely describe the analogue model. Therefore, the subsequent work is solely based on these quantities.

In Chapter 4, the analogue models developed in Chapter 3 are interpolated, with the help of a parametrization. The analogous model to a Schwarzschild black hole solution is interpolated to the analogue of an original analytic extension of an Ellis type of a Morris-Thorne wormhole, using a real parameter β. This parameter describes which model we are dealing with: $\beta = 0$ describes the Schwarschild case, while $\beta = 1$ describes the Morris-Thorne case. Other (unknown) models then emerge by taking values of β all along the real line (extrapolation). The results of the parametrization are presented as a numerical analysis of the generated class of models.

Chapter 5 collects the conclusions, together with a few devised future perspectives and developments this work may have. After the bibliographic list of references, Appendix A provides the relevant material for the proposed analytic extension of Morris-Thorne wormhole solution to the so called "internal region"; while Appendix B presents the

Mathematica$^{\text{TM}\text{®}\text{©}}$ code for the numerical analysis performed in Chapter 4.

Geometric units are employed throughout (such that the speed of light in vacuum is $c = 1$ and Newtonian gravitational constant is $G = 1$), and spacetimes are taken as Lorentzian geometries with $(+ - - -)$ signature. Einstein convention on implicit sums over repeated indices is assumed and comma $(,)$ represents partial derivative with respect to the spacetime coordinates: $X_{,\mu} := \partial_\mu X$.

Chapter 2

Gravitational solutions and the theory of electromagnetic analogue models

In this chapter, the basics for the development of this work is presented: Karl Schwarzschild obtained a gravitational solution representing a spherically symmetric black hole (in 1916), while Michael S. Morris and Kip S. Thorne obtained a solution describing a wormhole (in 1987). After the review on the two gravitational solutions, the mathematic theory behind the electromagnetic analogue models (in terms of Hadamard's approach to deal with abruptly varying fields) is discussed.

2.1 Gravitational solutions

2.1.1 Schwarzschild solution

The Schwarzschild solution was proposed in 1916 [8] as the first exact solution to the Einstein field equations. These field equations are composed by 10 coupled non-linear second order partial differential equations, which renders the analytical resolution process rather impractical. Schwarzschild's proposal consists of a very simple physical system: a static (and stationary), massive, electrically neutral, spherically symmetric body deprived

of rotation. This model is a paradigm, and brings forward the mathematical concept of a black hole.

Schwarzschild proposed that the spacetime metric should have coefficients that depend only on the radial coordinate r, due to sphericall symmetry. Therefore, he proposed the most general static spherically symmetric form for the spacetime invariant line element as [9]

$$\mathrm{d}s^2 = A(r)\,\mathrm{d}t^2 - B(r)\,\mathrm{d}r^2 - r^2\,\mathrm{d}\theta^2 - r^2\sin^2\theta\,\mathrm{d}\phi^2. \tag{2.1}$$

The functions $A(r)$ and $B(r)$ are obtained by solving Einstein equations in empty space and comparing with Newtonian gravity in the limit of large distances $r \to \infty$ (the Newtonian limit). In this way, Schwarzschild found

$$\mathrm{d}s^2_{(S)} = \left(1 - \frac{2M}{r}\right)\mathrm{d}t^2 - \left(1 - \frac{2M}{r}\right)^{-1}\mathrm{d}r^2 - r^2\,\mathrm{d}\theta^2 - r^2\sin^2\theta\,\mathrm{d}\phi^2. \tag{2.2}$$

From the theory of general relativity, the metric of spacetime can be read from the line element, since $\mathrm{d}s^2 = g_{\mu\nu}dx^\mu dx^\nu$. Therefore, Schwarzschild metric in matrix form reads

$$g^{(S)}_{\mu\nu} = \begin{pmatrix} 1 - \dfrac{2M}{r} & 0 & 0 & 0 \\ 0 & -\left(1 - \dfrac{2M}{r}\right)^{-1} & 0 & 0 \\ 0 & 0 & -r^2 & 0 \\ 0 & 0 & 0 & -r^2\sin^2\theta \end{pmatrix}. \tag{2.3}$$

Schwarzschild solution was important not only because it was the first solution to Einstein field equations, but also because it predicted the existence of black holes. According to the theory of general relativity, gravity is the effect from the deformation of spacetime, so that a massive body will distort spacetime so strongly as it is shown in Figure 2.1. This geometry has a limit at which nothing can escape its gravitational pull. This limit is called the event horizon and, for Schwarzschild solution, its value is $r = R$ where

$$R = 2M. \tag{2.4}$$

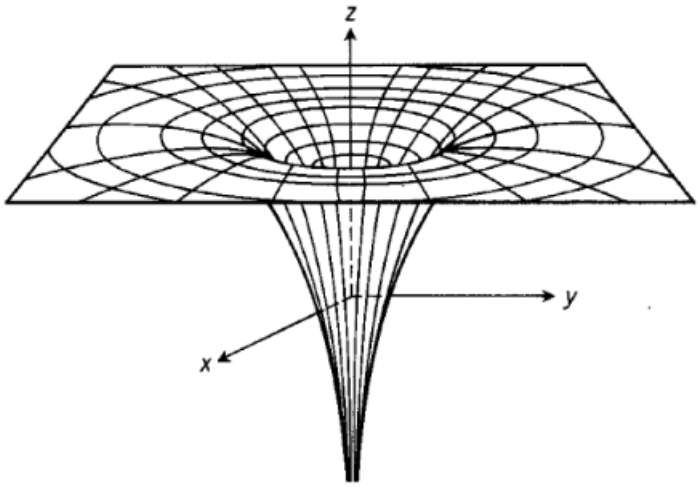

Figure 2.1: Spacetime deformation by a massive compact object. For the sake of easy visualization, spacetime is here depicted as a surface, and its Schwarzschild radius (the event horizon) appears as a circunpherence line in the diagram. (Reproduced [10] without permission).

It is apparent from Equation (2.2) that this geometry has two singularities: one at $r = R$, (that is, where the coordinate r is equal to the 'radius' R of the event horizon), and another at $r = 0$. The singularity at $r = R$ is removable, that is, the singularity disappears when another coordinate system is employed, so this singularity is not physical in status, but merely a mathematical one. The singularity presented in $r = 0$ is physical, that is, it cannot be removed by changing coordinates whatsoever, since there are scalar invariants (such as $R^{\alpha\beta\mu\nu}R_{\alpha\beta\mu\nu}$) which diverge at $r = 0$. No scalar invariant of Schwarzschild geometry diverge at the event horizon $r = R$.

2.1.2 Morris-Thorne Solution

Michael S. Morris and Kip S. Thorne developed a solution in 1987 [11], which describes what is called a wormhole. The standard analytic extension of such structure is shown in Figure 2.2. There is still no experimental evidence to support the existence of wormholes in the real world; however, the theory of general relativity predicts their existence in nature.

Morris-Thorne presented a metric for the description of wormholes, so that the line

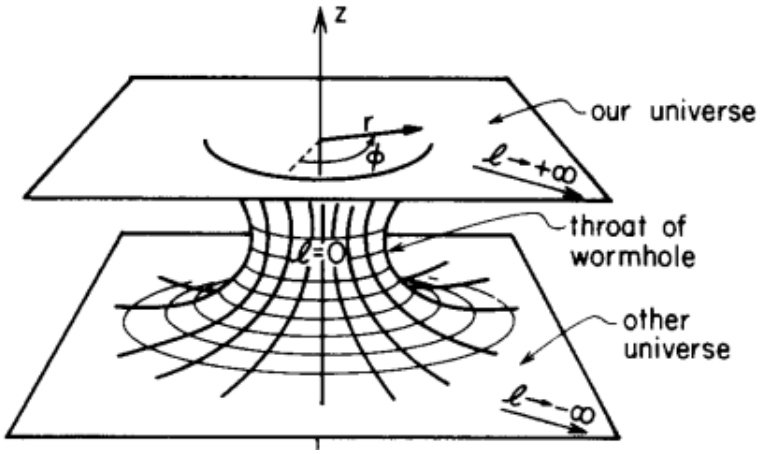

Figure 2.2: Basic diagram of a wormhole. Spacetime is depicted as a 2D surface for visualization purposes. The wormhole is a structure formed by two "mouths" connected by a "throat", so that two different far appart regions of the universe can be connected to one another, allowing matter to fastly travel back and forth between them. Parameter l measures the "distance" from the wormhole throat. (Reproduced [11] without permission.)

element in spherical coordinates is [11]

$$\mathrm{d}s^2_{(MT)} = e^{2\Phi(r)}\mathrm{d}t^2 - \left[1 - \frac{b(r)}{r}\right]^{-1}\mathrm{d}r^2 - r^2\,\mathrm{d}\theta^2 - r^2\sin^2\theta\,\mathrm{d}\phi^2, \tag{2.5}$$

where $b(r)$ and $\Phi(r)$ are functions to be determined. The $b(r)$ function determines the spatial shape of the wormhole, thus usually called "shape function" while $\Phi(r)$ determines the gravitational redshift, thus called the "redshift function" (more informations about $\Phi(r)$ and $b(r)$ can be found in the literature [12]). Given the expression of the invariant line element presented in Equation (2.5), the matrix form of the Morris-Thorne metric is

$$g^{(MT)}_{\mu\nu} = \begin{pmatrix} e^{2\Phi(r)} & 0 & 0 & 0 \\ 0 & -\left[1 - \frac{b(r)}{r}\right]^{-1} & 0 & 0 \\ 0 & 0 & -r^2 & 0 \\ 0 & 0 & 0 & -r^2\sin^2\theta \end{pmatrix}. \tag{2.6}$$

The Morris-Thorne metric and the Schwarzschild metric present two identical corresponding components ($g^{(S)}_{22} = g^{(MT)}_{22}$ and $g^{(S)}_{33} = g^{(MT)}_{33}$).

The two presented solutions are of great importance in the development of this work.

When one seeks an analogous model, it is necessary to define to which gravitational object the analogy is intended. In this work, the analogue models of both Schwarzschild and Morris-Thorne solutions are recalled from the literature [13, 14]. The present work provides generalizations and unification of these two models in one single family of analogue models (or, at least, of presumably analogue models).

2.2 Electromagnetic analogue models

In this section, the theory about analogue models is presented in order to obtain the effective metric for the optical problem. Initially, Maxwell electrodynamics is briefly presented, together with the constitutive relations, responsible for the description of the eventually nonlinear character of the theory. Then, a brief presentation of Hadamard method is given, under the hupothesis that the light propagation in the material medium takes place in the regime of geometrical optics. Finally, the optical effective metric is formally obtained.

2.2.1 Nonlinear electrodynamics

Maxwell electromagnetic theory is described by a set of four 3-vector partial differential equations, which determines the behavior of the electric $\vec{E}$ and magnetic $\vec{B}$ fields, as well as their respective inductions $\vec{D}$ (electric displacement) and $\vec{H}$ (magnetic induction). Maxwell's equations, which are usually presented in vector notation

$$\vec{\nabla}\cdot\vec{D} = 4\pi\rho, \tag{2.7}$$

$$\vec{\nabla}\cdot\vec{B} = 0, \tag{2.8}$$

$$\vec{\nabla}\times\vec{E}+\partial_t\vec{B} = 0, \tag{2.9}$$

$$\vec{\nabla}\times\vec{H}-\partial_t\vec{D} = 4\pi\vec{J}, \tag{2.10}$$

can be rewritten in partially covariant form; that is, covariant upon linear transformations of coordinates. Thus, the four vector Equations (2.7)–(2.10) are reduced to two tensor-like

equations in flat Minkowski spacetime, which are [15]

$$\partial_\mu P^{\mu\nu} = 4\pi\, J^\nu, \tag{2.11}$$

$$\partial_\mu N^{\mu\nu} = 0, \tag{2.12}$$

where $P^{\mu\nu}$ is the anti-symmetric polarization tensor, to be defined in Equation (2.16), while $J^\nu = (\rho, \vec{J})$ is the current density 4-vector, and $N^{\mu\nu}$ is the dual of the Faraday tensor $F^{\mu\nu}$, defined by

$$N^{\mu\nu} = \frac{1}{2}\eta^{\mu\nu}{}_{\alpha\beta}F^{\alpha\beta}, \tag{2.13}$$

where $\eta^{\mu\nu}{}_{\alpha\beta}$ is the Levi-Civita pseudo-tensor defined as

$$\eta_{\mu\nu\alpha\beta} = \sqrt{-\eta}\ \epsilon_{\mu\nu\alpha\beta}, \tag{2.14}$$

where η is the determinant of the Minkowski metric and $\epsilon_{\mu\nu\alpha\beta}$ is the Levi-Civita symbol. The tensors $F^{\mu\nu}$ and $P^{\mu\nu}$ can be specified with the help of a normalized time-like vector field v_μ (the four-velocity vector of the observer) comoving with the laboratory, as [16]

$$F^{\mu\nu} = E^\mu v^\nu - E^\nu v^\mu + \eta^{\mu\nu}{}_{\alpha\beta}B^\alpha v^\beta, \tag{2.15}$$

$$P^{\mu\nu} = D^\mu v^\nu - D^\nu v^\mu + \eta^{\mu\nu}{}_{\alpha\beta}H^\alpha v^\beta, \tag{2.16}$$

where by a time-like quadrivector field v^μ is meant $v_\mu v^\mu > 0$, and by normalized is meant $|v_\mu v^\mu| = 1$. The electromagnetic fields and the observer vector field satisfy

$$v^\mu E_\mu = 0, \quad v^\mu B_\mu = 0, \quad v^\mu D_\mu = 0, \quad v^\mu H_\mu = 0, \tag{2.17}$$

that is, the electromagnetic fields and their corresponding inductions are all space-like vectors. That is, they all have negative quadratic norms

$$E^\mu E_\mu = -E^2, \quad B^\mu B_\mu = -B^2, \quad D^\mu D_\mu = -D^2, \quad H^\mu H_\mu = -H^2. \tag{2.18}$$

The fundamental fields and their inductions are related by the constitutive relations

$$D_\lambda = \epsilon_\lambda{}^\nu E_\nu, \tag{2.19}$$

$$H_\lambda = (\mu^{-1})_\lambda{}^\nu B_\nu. \tag{2.20}$$

The constitutive relations determine the degree of nonlinearity of the theory, and this depends on the behavior of the electric permittivity $\epsilon_\lambda{}^\nu$ and magnetic permeability $\mu_\lambda{}^\nu$. If both these quantities take constant values, the corresponding electrodynamic theory is said to be linear; otherwise, it is then said to be nonlinear (that is, with these quantities eventually being depend on the field intensity). More aspects regarding nonlinearity can be found in the literature [17]. In order to obtain the effective metric, a very simple nonlinear case, in which the magnetic permeability is taken to be constant value (equal to μ_0 of vacuum), and the electric permittivity is a function of the intensity of the electric field E only. In this way, the constitutive relations for the proposed material medium read

$$D_\lambda = \epsilon(E) E_\lambda, \tag{2.21}$$

$$H_\lambda = \frac{1}{\mu_0} B_\lambda. \tag{2.22}$$

Such constitutive relations are then inserted in Equations (2.11) and (2.12), in order to obtain the effects of nonlinearity of the material medium.

2.2.2 Hadamard method for abruptly varying fields

The Hadamard method [18] is an important tool regarding the study of light propagation. It amounts to calculate the step (or "leap") that some functions may present, when evaluated at both sides of a distinguished hypersurface Σ (in this case, the hypersurface is the wave-front) [19]. Although the system being dealt with is electromagnetic, the method is valid for more general contexts (more about the Hadamard method can be found in the literature [20]).

Let Σ_t be a 2-dimensional surface that delimits two disjoint regions as shown in Fi-

gure 2.3. Such a surface is the instantaneous projection at time t of the mentioned hypersurface Σ onto 3-space, and is called the wave-front.

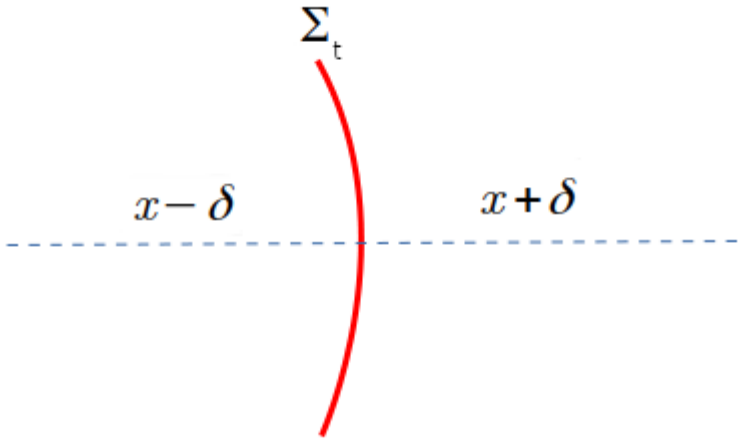

Figure 2.3: Σ_t is the instantaneous (wave-front) hypersurface which separates two globally defined disjoint regions: $x - \delta$ represents the region in which that surface Σ_t has passed already, while $x + \delta$ represents the region in which that surface Σ_t is still arrive.

The method then evaluates the step of any physical tensor quantity Z across the hypersurface Σ as

$$[Z(x)]_\Sigma := \lim_{\delta \to 0^+} [Z(x+\delta) - Z(x-\delta)]. \tag{2.23}$$

Hadamard showed that, if $[Z(x)]_\Sigma = 0$, then necessarily there exists a tensor $\bar{f}$ with the same rank of $Z(x)$, and satisfying the same algebraic identities as $Z(x)$, such that $[\partial_\nu Z(x)]_\Sigma = \bar{f} k_\nu$, where k_ν is everywhere orthogonal to Σ. If the hypersurface Σ is given by $\phi(x) = 0$, then $k_\nu = \nabla_\nu \phi$. That is, the gradient of any zero-step quantity across Σ has a step across Σ which must be proportional to the wave vector k_ν.

Care should be taken with the possible confusion between step and "discontinuity". Since nothing has been said about the function $\partial_\nu Z$ at Σ [21].

Therefore, this method can be applied to the fields E_μ and B_μ. Considering that the fields have no step across the hypersurface Σ (that is, $[E_\mu]_\Sigma = 0$ and $[B_\mu]_\Sigma = 0$), then Hadamard theorem yields

$$[\partial_\nu E_\mu]_\Sigma = e_\mu k_\nu, \tag{2.24}$$

$$[\partial_\nu B_\mu]_\Sigma = b_\mu k_\nu, \tag{2.25}$$

where e_μ and b_μ are space-like vector fields which carry all the information on the polarization of the E_μ and B_μ fields, respectively.

2.2.3 The optical effective metric

Suppose a material medium with nonlinear electromagnetic behavior. The problem is that of light propagation inside such medium in the limit of small wave-lenghts (known as geometrical optics limit), described with the aid of Hadamard's approach. The resulting dispersion relation is expressed as an effective optical metric. Initially, the dual tensor $N^{\mu\nu}$ is expressed as a function of the electric E^μ and magnetic B^μ fields from Equations (2.13) and (2.15). With the help of the identity $\eta_{\mu\nu\alpha\beta}\eta^{\alpha\beta\rho\sigma} = 2(\delta^\rho_\nu\delta^\sigma_\mu - \delta^\rho_\mu\delta^\sigma_\nu)$, this tensor reads

$$N^{\mu\nu} = B^\mu v^\nu - B^\nu v^\mu + \eta^{\mu\nu}{}_{\alpha\beta}E^\alpha v^\beta. \tag{2.26}$$

The Substitution of tensors $P^{\mu\nu}$ and $N^{\mu\nu}$ from Equations (2.16) and (2.26) in Maxwell Equations (2.11) and (2.12) yields

$$D^\mu{}_{,\mu}\, v^\nu + D^\mu v^\nu{}_{,\mu} - D^\nu{}_{,\mu}\, v^\mu + D^\nu v^\mu{}_{,\mu} + \eta^{\mu\nu}{}_{\alpha\beta}(H^\alpha{}_{,\mu}\, v^\beta + H^\alpha v^\beta{}_{,\mu}) = 4\pi\, J^\nu, \tag{2.27}$$

$$B^\mu{}_{,\mu}\, v^\nu + B^\mu v^\nu{}_{,\mu} - B^\nu{}_{,\mu}\, v^\mu + B^\nu v^\mu{}_{,\mu} + \eta^{\mu\nu}{}_{\alpha\beta}(E^\alpha{}_{,\mu}\, v^\beta + E^\alpha v^\beta{}_{,\mu}) = 0. \tag{2.28}$$

For the sake of simplicity of this work, it is assumed that $v^\mu{}_{,\nu} = 0$, which means that the 4-velocity of the observer does not vary throughout spacetime. With this simplification, Equations (2.27) and (2.28) read

$$D^\mu{}_{,\mu}\, v^\nu - D^\nu{}_{,\mu}\, v^\mu + \eta^{\mu\nu}{}_{\alpha\beta}H^\alpha{}_{,\mu}\, v^\beta = 4\pi\, J^\nu, \tag{2.29}$$

$$B^\mu{}_{,\mu}\, v^\nu - B^\nu{}_{,\mu}\, v^\mu + \eta^{\mu\nu}{}_{\alpha\beta}E^\alpha{}_{,\mu}\, v^\beta = 0. \tag{2.30}$$

The contraction of Equations (2.29) and (2.30) with v_ν yields scalar equations

$$(\epsilon\, E^\mu)_{,\mu}\, v^\nu v_\nu - (\epsilon\, E^\nu)_{,\mu}\, v^\mu v_\nu + \frac{1}{\mu_0}\eta^{\mu\nu}{}_{\alpha\beta}B^\alpha{}_{,\mu}\, v^\beta v_\nu = 4\pi\, J^\nu v_\nu, \tag{2.31}$$

$$B^{\mu}{}_{,\mu}\, v^{\nu} v_{\nu} - B^{\nu}{}_{,\mu}\, v^{\mu} v_{\nu} + \eta^{\mu\nu}{}_{\alpha\beta} E^{\alpha}{}_{,\mu}\, v^{\beta} v_{\nu} = 0. \tag{2.32}$$

The terms that involve $\eta^{\mu\nu}{}_{\alpha\beta} v^{\beta} v_{\nu}$ vanish. That is $\eta^{\mu\nu}{}_{\alpha\beta}$ is antisymmetric upon the interchange of the indices β and ν, while the product $v^{\beta} v_{\nu}$ is symmetric. Equations (2.31) and (2.32) read

$$\epsilon\, E^{\nu}{}_{,\nu} + \epsilon' \frac{E^{\alpha} E^{\nu}}{E} E_{\alpha,\nu} = 4\pi\, J^{\nu} v_{\nu}, \tag{2.33}$$

$$B^{\nu}{}_{,\nu} = 0, \tag{2.34}$$

where the prime (') in Equation (2.33) refers to the ordinary derivative with respect to the argument, which in this case is the magnitude E of the electric field.

On the other hand, contraction of Equations (2.29) and (2.30) with the projector $h^{\mu\nu} = \eta^{\mu\nu} - v^{\mu} v^{\nu}$ onto the 3-space which is orthogonal to the observer v^{μ} gives

$$-\epsilon \dot{E}^{\lambda} - \frac{\epsilon' E^{\mu} v^{\alpha} E_{\mu,\alpha}}{E} E^{\lambda} + \frac{1}{\mu_0} v_{\rho} B_{\sigma,\beta}\, \eta^{\lambda\beta\rho\sigma} = 4\pi\, J_{\gamma} h^{\gamma\lambda}, \tag{2.35}$$

$$\dot{B}^{\lambda} + v_{\rho} E_{\sigma,\beta}\, \eta^{\lambda\rho\sigma\beta} = 0, \tag{2.36}$$

where $\dot{E}^{\lambda}$ means partial derivative of E^{λ} with respect to the time coordinate t (and similarly for $\dot{B}^{\lambda}$).

Equations (2.33)–(2.36) completely describe the electrodynamics inside the proposed material medium. The induced optics, in the limit of small wave-lenghts known as geometrical optics, can be obtained from these equations with the help of the Hadamard method set in Section 2.2.2. The step of Equations (2.33)–(2.36) across the hypersurface Σ shall then be evaluated. The step of Equation (2.33) is

$$\epsilon [E^{\nu}{}_{,\nu}]_{\Sigma} + \epsilon' \frac{E^{\alpha} E^{\nu}}{E} [E_{\alpha,\nu}]_{\Sigma} = 4\pi\, [J^{\nu}]_{\Sigma}\, v_{\nu}. \tag{2.37}$$

With the use of Equation (2.24), and assuming that

$$[J^{\nu}]_{\Sigma} = 0, \tag{2.38}$$

Equation (2.37) then gives

$$\epsilon e^{\alpha} k_{\alpha} + \frac{e'}{E} E^{\alpha} E^{\beta} e_{\alpha} k_{\beta} = 0. \tag{2.39}$$

The step of Equation (2.34) is

$$[B^{\nu}{}_{,\nu}]_{\Sigma} = 0, \tag{2.40}$$

reduced, with the help of Equation (2.25), to

$$b^{\alpha} k_{\alpha} = 0. \tag{2.41}$$

The step of Equation (2.35)

$$-\epsilon[\dot{E}^{\lambda}]_{\Sigma} - \frac{\epsilon'}{E} E^{\mu} v^{\alpha} E^{\lambda} [E_{\mu,\alpha}]_{\Sigma} + \frac{1}{\mu_0} v_{\rho} \eta^{\lambda\beta\rho\sigma} [B_{\sigma,\beta}]_{\Sigma} = 4\pi \, [J_{\gamma}]_{\Sigma} \; h^{\gamma\lambda}, \tag{2.42}$$

can be rewritten with the help of

$$\dot{E}^{\lambda} = \frac{\partial E^{\lambda}}{\partial t} = v^{\nu} E^{\lambda}{}_{,\nu} \,, \tag{2.43}$$

the step evaluation of which is $[\dot{E}^{\lambda}]_{\Sigma} = e^{\lambda} k_{\nu} v^{\nu}$. Therefore

$$\epsilon e^{\lambda} k_{\nu} v^{\nu} + \frac{\epsilon'}{E} v^{\alpha} E^{\mu} E^{\lambda} e_{\mu} k_{\alpha} - \frac{1}{\mu_0} \eta^{\lambda\beta\rho\sigma} v_{\rho} b_{\sigma} k_{\beta} = 0. \tag{2.44}$$

Finally, the step of Equation (2.36) is

$$[\dot{B}^{\lambda}]_{\Sigma} + \eta^{\lambda\beta\rho\sigma} v_{\rho} [E_{\sigma,\beta}]_{\Sigma} = 0, \tag{2.45}$$

reduced from Equations (2.24) and (2.25) to

$$b^{\lambda} k_{\nu} v^{\nu} + \eta^{\lambda\beta\rho\sigma} v_{\rho} e_{\sigma} k_{\beta} = 0. \tag{2.46}$$

For $k_{\lambda} v^{\lambda} \neq 0$, Equations (2.39) and (2.41) can be obtained by Equations (2.44) and (2.46). Therefore, Equations (2.44) and (2.46) form a set which completely describes the behavior

and propagation of the wave vector k_μ.

Effective optical metrics for the problem can be obtained from the set of Equations (2.44) and (2.46). Equation (2.46) can be solved for b_λ as

$$b_\lambda = -\frac{\eta_\lambda{}^{\beta\rho\sigma} v_\rho e_\sigma k_\beta}{k_\nu v^\nu}, \tag{2.47}$$

thus rendering evident the linear polarization of the propagating light-ray. Substitution of Equation (2.47) in Equation (2.44) gives

$$\mu_0 \epsilon v^\mu k_\mu e^\lambda + \frac{\mu_0 \epsilon'}{E} v^\alpha k_\alpha E^\mu e_\mu E^\lambda + \frac{1}{v^\mu k_\mu} v_\rho v_\phi k_\beta k_\gamma e_\delta \eta^{\lambda\beta\rho}{}_\alpha \eta^{\alpha\gamma\phi\delta} = 0. \tag{2.48}$$

The above equation presents a term with the product $\eta^{\lambda\beta\rho}{}_\alpha \eta^{\alpha\gamma\phi\delta}$. The product can be expressed as a function of the metric $\eta^{\mu\nu}$ with the help of the identity [22]

$$\eta_{\zeta\nu\sigma\alpha}\eta^{\gamma\phi\delta\alpha} = \delta^\gamma_\nu(\delta^\phi_\zeta\delta^\delta_\sigma - \delta^\phi_\sigma\delta^\delta_\zeta) + \delta^\gamma_\zeta(\delta^\phi_\sigma\delta^\delta_\nu - \delta^\phi_\nu\delta^\delta_\sigma) + \delta^\gamma_\sigma(\delta^\phi_\nu\delta^\delta_\zeta - \delta^\phi_\zeta\delta^\delta_\nu). \tag{2.49}$$

By substituting Equation (2.49) in Equation (2.48), it can be shown that this term becomes

$$v_\rho v_\phi k_\beta k_\gamma e_\delta \eta^{\lambda\beta\rho}{}_\alpha \eta^{\alpha\gamma\phi\delta} = k^\nu k_\nu e^\lambda - k^\nu k^\lambda e_\nu + k^\nu k_\sigma v^\sigma (e_\nu v^\lambda - v_\nu e^\lambda). \tag{2.50}$$

Equation (2.48) similarly reduces to

$$\epsilon v^\nu k_\nu e^\lambda + \frac{\epsilon'}{E} v^\alpha k_\alpha E^\mu e_\mu E^\lambda + \frac{e^\lambda[k^\nu k_\nu - (k^\nu v_\nu)^2] - k^\nu e_\nu k_\sigma h^{\sigma\lambda}}{\mu_0 v^\beta k_\beta} = 0. \tag{2.51}$$

On the other hand, from Equation (2.39), the contraction $e^\nu k_\nu$ can be eliminated in terms of $e_\alpha E^\alpha E^\beta k_\beta$, and substitution of this in Equation (2.51) yields Fresnel eigenvalue Equation (2.52)

$$Z^\alpha{}_\beta e^\beta = 0, \tag{2.52}$$

where $Z^\alpha{}_\beta$ is known as generalized Fresnel matrix [23] and, which can be expressed as a

function of the normalized vector $l^\mu = E^\mu/E$ as

$$Z^\alpha{}_\beta = \epsilon(\delta^\alpha_\beta - v^\alpha_\beta) - \epsilon' E l^\alpha l_\beta - \frac{1}{\mu_0 {v_{ph}}^2}\left(\delta^\alpha_\beta - v^\alpha v_\beta - \frac{h^{\alpha\mu}k_\mu h_{\beta\nu}k^\nu}{h^{\rho\sigma}k_\rho k_\sigma}\right), \tag{2.53}$$

where $v_{ph} = 1/\sqrt{\mu\epsilon}$. Non-trivial solutions of the eigenvalue Equation (2.52) require a degenerate spatial projection of Fresnel matrix $Z^\alpha{}_\beta$ as

$$\det_{(3)} Z^\alpha{}_\beta = 0. \tag{2.54}$$

Equation (2.54) has two solution known as the ordinary mode and the extraordinary mode. The ordinary mode is described by the Gordon metric [24]

$$\tilde{g}^{\rho\beta} = v^\rho v^\beta(\mu_0\epsilon - 1) + \eta^{\rho\beta}, \tag{2.55}$$

and the extraordinary mode is described by generalized Gordon metric

$$\tilde{g}^{\rho\beta} = v^\rho v^\beta(\mu_0\epsilon + \mu_0\epsilon' E - 1) + \eta^{\rho\beta} - \frac{\epsilon'}{\epsilon E}E^\beta E^\rho, \tag{2.56}$$

where $\eta^{\rho\beta}$ is the Minkowski metric of the flat spacetime.

The focus of this work regards solely the extraordinary mode represented in Equation (2.56). This equation involves the matrix inverse (or contravariant) of the effective metric of the problem. In order to get the (covariant) effective metric, one just needs to solve for $\tilde{g}_{\nu\rho}$ in the equation

$$\tilde{g}^{\mu\nu}\tilde{g}_{\nu\rho} = \delta^\mu_\rho. \tag{2.57}$$

The solution of Equations (2.56) and (2.57) for the optical effective metric is

$$\tilde{g}_{\mu\nu} = \eta_{\mu\nu} - \left[1 - \frac{1}{\mu_0\epsilon(\xi+1)}\right]v_\mu v_\nu + \left(\frac{\xi}{\xi+1}\right)l_\mu l_\nu, \tag{2.58}$$

where $\xi = E\epsilon'/\epsilon$.

Equation (2.58) gives the mathematical description of the propagation of the light-ray with the extraordinary polarization inside the dielectric material. The explicit construc-

tion of the optical analogue models of interest from it are presented in Chapter 3.

Chapter 3

Analogue models for Schwarzschild and Morris-Thorne

With the effective metric at hand, as obtained in Chapter 2, the optical analogue models of interest can be built. This chapter is dedicated to the construction and discussion of an analogous model of the analytically extended Schwarschild black hole, and of an analogous model of the somehow analytically extended Ellis type of Morris-Thorne wormhole. Both are partially known in the literature: the extended Schwarzschild model is known [14] for a different constitutive relation $\mu \sim \epsilon^{-3}$, while the standard Ellis model [25] of a Morris-Thorne wormhole is endowed here with an original analytic extension.

3.1 Analogue model for the Schwarzschild black hole

The effective metric can be compared with different geometries, in order to obtain the corresponding analogous model. This comparison is valid due to the discussion presented in Chapter 2, since the light beam propagates within the material medium along effectively null lines[1]. The effective metric, determined from Equation (2.58) can be expressed in

[1]With respect to the effective metric, such curve lines are not only null (or light-like) in character, but also geodesics in nature [26].

components as the diagonal matrix

$$\tilde{g}_{\mu\nu} = \text{diag}\left(\mu_0(\epsilon + \epsilon' E), -\frac{\epsilon + \epsilon' E}{\epsilon}, -\frac{1}{r^2}, -\frac{1}{r^2 \sin^2\theta}\right), \tag{3.1}$$

that can be compared directly with the Schwarzschild black hole metric

$$g_{\mu\nu} = \text{diag}\left(A, -\frac{1}{A}, -r^2, -r^2 \sin^2\theta\right), \tag{3.2}$$

where $A = A(r) = 1 - R/r$, with R being the gravitational (Schwarzschild) radius[2] of the black hole.

The comparison is made by matching each component of the effective metric with the corresponding component of the metric of interest. In this case, the non-trivial matching equations are

$$\tilde{g}_{00} = g_{00}, \quad \tilde{g}_{11} = g_{11}, \quad \tilde{g}_{22} = g_{22}, \quad \tilde{g}_{33} = g_{33}. \tag{3.3}$$

Such comparisons relate the electromagnetic quantities (derived from the effective metric) to the gravitational quantities (derived from the black hole metric). The result is [14]

$$E = \frac{E_0 R}{|r - R|}, \tag{3.4}$$

$$\rho = \frac{\epsilon_0 E_0 R}{r^2}, \tag{3.5}$$

$$D = \frac{\epsilon_0 E_0 R}{r}, \tag{3.6}$$

$$\epsilon = \epsilon_0 \left|1 - \frac{R}{r}\right|, \tag{3.7}$$

where E_0 is the strength E of electric field evaluated at $r = r_0$, with r_0 being any given positive constant. Equations (3.4)–(3.7) were obtained in the literature [14] using the fact that the magnetic permeability has a functional dependence $\mu \sim \epsilon^{-3}$. However, the results in Equations (3.4)–(3.7) can be utilized here because the fundamental interest is to analyze the electromagnetic quantities near the horizon R and, around it, all the observable fields

[2]The standard nomenclature of "Schwarzschild radius" for the singular value of the radial coordinate r is rather misleading, since this coordinate r measures the lenght of circunpherences but not their radii. The expression "radial coordinate", when applied to such r, is similarly misleading.

(i.e., the electric displacement D and the electric density of charge ρ, aside from the magnetic induction H_λ) present a regular behavior in the horizon, and Equations (3.4)–(3.7) can be used. The electromagnetic quantities presented in Equations (3.4)–(3.7) above provide a direct relationship between the gravitational model and the optical model analogous to it. All of these quantities are expressed in terms of the "radial" coordinate r, having the value of the "radius" of the event horizon denoted by R. Note that the equations are valid for both internal $r < R$ and external $r > R$ regions. Another important feature is the functional dependence of the electromagnetic quantities, all of which are functions of the "radial" coordinate r only (due to spherical symmetry of the material medium). That is, the problem is strictly radial. In this way, the material medium being dealt with must display spherical symmetry.

3.2 Analogue model for the Morris-Thorne wormhole

An analogous model of the Morris-Thorne wormhole can similarly be constructed, upon comparison of the effective metric from Equation (3.1) with the metric of interest

$$g_{\mu\nu} = \text{diag}\left[e^{2\Phi(r)}, -\left(1-\frac{b(r)}{r}\right)^{-1}, -r^2, -r^2\sin^2\theta\right]. \tag{3.8}$$

Simplifying choices can be applied to the metric above. Such choices involve the quantities $\Phi(r)$ and $b(r)$, which were presented in Chapter 2.

A Gaussian time coordinate t can be used for simplicity, which means

$$\Phi(r) = 0. \tag{3.9}$$

Regarding $b(r)$, it is here assumed the Ellis model [25]

$$b(r) = \frac{n^2}{r}, \tag{3.10}$$

where n is the minimum lenght for the r coordinate from within the accessible region of the wormhole (we shall call n as the "minimum radius" of the wormhole for brevity,

despite the fact that it is not a radial measure).

With these restrictions for $\Phi(r)$ and $b(r)$, the Morris-Thorne metric Equation (3.8) reads

$$g_{\mu\nu} = \text{diag}\left[1, -\left(1 - \frac{n^2}{r^2}\right)^{-1}, -r^2, -r^2\sin^2\theta\right]. \tag{3.11}$$

It is worth to stress that, in Equation (3.11), the radial coordinate r is defined only for values $r > n$, that is, for values of r larger than the minimum radius n; this spacetime region is here termed as the "external" region. Equation (3.11) give the functional form for the gravitational potential as $V \sim r^{-2}$ in Ellis type of Morris-Thorne model. The Raissner-Nordström model [27] has the same functional form for the gravitational potential for the Coulomb interaction (that is, by formally dropping out the term of mass in this model); however, with the opposite sign.

3.2.1 External Region $r > n$

Since the Morris-Thorne metric from Equation (3.11) is valid only for the external region $r > n$, the electromagnetic analogue quantities are defined only in this region. A direct comparison between the effective metric and the gravitational metric yields [13]

$$\frac{\epsilon}{\epsilon_0} = \frac{1}{1+\xi}, \tag{3.12}$$

$$\xi = -\frac{n^2}{r^2}. \tag{3.13}$$

Equations (3.12) and (3.13) above specify the electric permittivity ϵ as a function of the radial coordinate r:

$$\epsilon(r) = \epsilon_0\left(\frac{r^2}{r^2 - n^2}\right). \tag{3.14}$$

Equation (3.13) is an ordinary first-order differential equation for the electric field, which can be easily solved in order to obtain the electric field $E(r)$, since

$$\xi = -\frac{n^2}{r^2} = \frac{E\epsilon'}{\epsilon} = \frac{E}{\epsilon}\frac{\mathrm{d}\epsilon}{\mathrm{d}E} = \frac{E}{\epsilon}\frac{\mathrm{d}\epsilon/\mathrm{d}r}{\mathrm{d}E/\mathrm{d}r}. \tag{3.15}$$

Thus, a simple substitution in Equation (3.15) of the explicit form for the total derivative of $\epsilon(r)$, which can be calculated from Equation (3.14), yields

$$\frac{\mathrm{d}E}{E} = \frac{2r}{r^2 - n^2}\mathrm{d}r. \tag{3.16}$$

The solution of Equation (3.16) for the electric field is

$$E(r) = E_0 \left(\frac{r^2 - n^2}{r_0^2 - n^2} \right), \tag{3.17}$$

where $r_0 > n$ is as an arbitrary integration constant called "accessible radius", and E_0 is the value of the electric field at $r = r_0$. The constitutive relation $D(r) = \epsilon(r)E(r)$ then yields the electric displacement as

$$D(r) = \frac{\epsilon_0 E_0 r^2}{(r_0^2 - n^2)}. \tag{3.18}$$

Consequently, the volumetric density of electric charges ρ is given by Gauss law

$$\vec{\nabla} \cdot \vec{D} = \frac{1}{r^2}\frac{\mathrm{d}}{\mathrm{d}r}\left[r^2 D(r)\right] = 4\pi\rho, \tag{3.19}$$

which gives

$$\rho(r) = \frac{\epsilon_0}{\pi}\left(\frac{E_0}{r_0^2 - n^2} \right) r. \tag{3.20}$$

This set of Equations (3.14), (3.17), (3.18) and (3.20) determine all four electromagnetic quantities which are important for the physical description of the optical analogue model. Recall that Equations (3.14), (3.17), (3.18) and (3.20) are valid only for the external region $r > n$ of the wormhole.

3.2.2 Internal Region $r < n$

The material provided in this section was not known in the literature.

The effective metric given in Equation (3.11) is only valid for the external region $r > n$. This work aims to compare the Schwarzschild analogue model with the Ellis type

of Morris-Thorne analogue model. However, the gravitational Schwarzschild geometry is valid in $r > 0$, while the gravitational geometry for Ellis type of Morris-Thorne is valid in $r > n$. Therefore, it is necessary to extend the Ellis type of Morris-Thorne model for $r > 0$. In order to achieve this goal, an analytic extension of the metric from Equation (3.11) is required, so that it can describe the whole $r > 0$ coordinate domain. A convenient analytic extension of the metric is

$$g_{\mu\nu} = \text{diag}\left[1, -\left|1 - \frac{n^2}{r^2}\right|^{-1}, -r^2, -r^2\sin^2\theta\right]. \tag{3.21}$$

See Appendix A for details. The metric in Equation (3.21) is expressed in a way that is valid for both external and internal regions, in complete similitude with Equation (3.2).

The analogue electromagnetic quantities are similarly obtained by direct comparison between the effective metric in Equation (3.1) and the extended Morris-Thorne metric in Equation (3.21) as

$$\frac{\epsilon}{\epsilon_0} = \frac{1}{1+\xi}, \tag{3.22}$$

$$\xi + 1 = \left|1 - \frac{n^2}{r^2}\right|, \tag{3.23}$$

so that the electric permittivity reads

$$\epsilon(r) = \epsilon_0 \left|1 - \frac{n^2}{r^2}\right|^{-1}. \tag{3.24}$$

The electric field $E(r)$ is then obtained from differential Equation (3.23). In the internal region, such differential equation becomes

$$\xi = \frac{n^2}{r^2} - 2 = \frac{E\epsilon'}{\epsilon} = \frac{E}{\epsilon}\frac{\mathrm{d}\epsilon}{\mathrm{d}E} = \frac{E}{\epsilon}\frac{\mathrm{d}\epsilon/\mathrm{d}r}{\mathrm{d}E/\mathrm{d}r}. \tag{3.25}$$

The total derivative with respect to the r coordinate of the electric permittivity ϵ is immediately determined by Equation (3.24). Therefore, Equation (3.25) gives

$$\frac{\mathrm{d}E}{E} = \frac{2rn^2}{(n^2 - r^2)(n^2 - 2r^2)}\mathrm{d}r, \tag{3.26}$$

from which the electric field is

$$E = E_0 \left(\frac{2r_0^2 - n^2}{r_0^2 - n^2} \right) \left(\frac{r^2 - n^2}{2r^2 - n^2} \right), \tag{3.27}$$

where $r_0 > n$ is as arbitrary integration constant. E_0 is the value of the external electric field at $r = r_0$ as described in Section 3.2.1. The electric displacement $D(r)$ is given by the constitutive relation as

$$D(r) = \epsilon_0 E_0 \left(\frac{2r_0^2 - n^2}{r_0^2 - n^2} \right) \left(\frac{r^2}{n^2 - 2r^2} \right). \tag{3.28}$$

In order to complete the set of electromagnetic quantities for the analogue model, Gauss law from Equation (3.19) yields

$$\rho = \frac{\epsilon_0 E_0}{\pi} \left(\frac{2r_0^2 - n^2}{r_0^2 - n^2} \right) \left[\frac{(n^2 - r^2)r}{(n^2 - 2r^2)^2} \right]. \tag{3.29}$$

Thus, all the four electromagnetic quantities for the analogue model are known at the internal region as well. Thus, with this generalization of the Ellis model for the Morris-Thorne metric, a more complete and general model was constructed than the one previously known in the literature [13]. Chapter 4 unifies these two analogue models developed so far: the model for a Schwarzschild black hole and the model for a Ellis type of a Morris-Thorne wormhole.

Chapter 4

Parametrization of analogue models

The aim of this chapter is to provide a unified view of the two analogue models worked out in Chapter 3, thus further generalizing these models. A real parametrization is provided, in order to obtain a family of physical systems which are here being proposed as candidates of analogue models. Some important features about the models become apparent from them, allowing one to address the fundamental question of the present work: how to measure the difference between (the analogues of) a black hole and a wormhole?

4.1 The parametrization of the models

The parametrization is presented as a form of unification between the optical analogue models that were described in this work. This unification provides a family described by a parameter β which can assume any real value. A whole new class of possibly analogue models emmerges as a result.

For the analogue of a Schwarzschild black hole, the electric permittivity is

$$\epsilon = \epsilon_0 \left| 1 - \frac{R}{r} \right|, \quad r > 0, \tag{4.1}$$

while for the analogue of the Ellis type of a Morris-Thorne wormhole, the electric permit-

tivity behaves as

$$\epsilon = \epsilon_0 \left| 1 - \frac{R^2}{r^2} \right|^{-1}, \quad r > 0, \tag{4.2}$$

where, for the sake of unification, it is convenient to define

$$R = n, \tag{4.3}$$

in Equation (4.2).

The proposal is to unify the electric permittivity from Equations (4.1) and (4.2) of these two models with the help of an arbitrary real parameter β. The correspondence $\beta = 0$ to Schwarzschild black hole and $\beta = 1$ to Morris-Thorne wormhole is arbitrarily adopted here. Therefore, a possible parametrization of Equations (4.1) and (4.2) is

$$\epsilon = \epsilon_0 \left| 1 - \left(\frac{R}{r} \right)^{1+\beta} \right|^{1-2\beta}. \tag{4.4}$$

Note that Equation (4.4) above reduces to Equation (4.1) for $\beta = 0$, and to Equation (4.2) for $\beta = 1$.

The same procedure yields the parametrization of the electric charge density ρ. For the analogue of a Schwarzschild black hole, one has

$$\rho = \frac{\epsilon_0 E_0 R}{r^2}, \quad r > 0, \tag{4.5}$$

where R is given by Equation (2.4) and, for the analogue of the Ellis type of a Morris-Thorne wormhole,

$$\rho = \begin{cases} \dfrac{\epsilon_0}{\pi} \left(\dfrac{E_0}{r_0^2 - R^2} \right) r, & r > R; \\ \\ \dfrac{\epsilon_0 E_0}{\pi} \left(\dfrac{2r_0^2 - R^2}{r_0^2 - R^2} \right) \left[\dfrac{(R^2 - r^2) r}{(R^2 - 2r^2)^2} \right], & r < R, \end{cases} \tag{4.6}$$

where R is given by Equation (4.3), and $r_0 > R$ is an integration constant to be determined from the boundary conditions. For the parametrization, the arbitrary choice $r_0 = 2R$ is

taken, in order to provide explicit calculations. Therefore, Equation (4.6) reduces to

$$\rho = \begin{cases} \dfrac{\epsilon_0 E_0}{3\pi R^2} r, & r > R; \\ \\ \dfrac{7\epsilon_0 E_0}{3\pi} \left[\dfrac{(R^2 - r^2) r}{(R^2 - 2r^2)^2} \right], & r < R. \end{cases} \tag{4.7}$$

Equations (4.5) and (4.7) can be parametrized as

$$\rho = \frac{\epsilon_0 E_0 r^{3\beta-2}}{(3\pi)^\beta R^{3\beta-1}} \left\{ 1 + \beta \Theta(R - r) \left[\frac{7R^2(R^2 - r^2)}{(R^2 - 2r^2)^2} - 1 \right] \right\}, \tag{4.8}$$

where $\Theta(R - r)$ is the Heaviside step function, defined as

$$\Theta(x) = \begin{cases} 0, & x < 0; \\ 1/2, & x = 0; \\ 1, & x > 0. \end{cases} \tag{4.9}$$

Note that Equation (4.8) above reduces to Equation (4.5) for $\beta = 0$, and to Equation (4.7) for $\beta = 1$. However, since Equations (4.4) and (4.8) were both imposed by hand, there is no *a priori* guarantee that the resulting system of equations is physically compatible.

The parametrization for the electric displacement D is given by Gauss law using the parametrized density of electric charge ρ, while the parametrization of the electric field E is then given from the use of the parametrized constitutive relation for D and ϵ. Thus, the set of Equations (4.4) and (4.8) is the focus of this work, and provides the unification of the two analogous models discussed in this work: Schwarzschild black hole and Morris-Thorne wormhole. In addition to unifying these two models, such set proposes the existence of a whole new family of optical models, since the parameter β can assume any real value.

Note that Equation (4.7) have a nonzero step at $r = R$. The presence of this non-zero step violates Equation (2.38), thus appearing to invalidate the provided analysis of the model. Fortunately, this is not the case, but only amounts to bother one with the need to deal with Dirac-delta distributions in the calculations: the resulting effective geometry is kept safely unchanged wherever Equation (2.38) is fulfilled — that is, almost everywhere

but at $r = R$.

The electric displacement $\vec{D}$ can be obtained from Gauss law expressed in Equation (3.19). Due to spherical symmetry, the magnitude D of the electric displacement vector field depends only on the radial coordinate. Thus, solving Gauss Equation (3.19) in this case is a simple task: the electric charge density can be integrated over 3-space in order to obtain the total electric charge. For such integration, the parametrized expression for the electric charge density from Equation (4.8) is used. Since this integration does not depend on the angular coordinates, the integral is

$$Q = 4\pi \int_0^r \rho(r')\ r'^2 dr', \tag{4.10}$$

for the function $Q = Q(r)$ which evaluates the total amount of electric charge enclosed by a sphere of area $4\pi r^2$. Explicit evaluation of the integral in Equation (4.10) can only be solved numerically, as it involves special functions. The numerically integrated expression formally diverges at $r = 0$, which is obviously inconsistent. In order to regularize such spurious divergence, it is proposed that the material medium of interest should have a small "hole" of radius x at its center; that is, it should be filled with another different material, in order to allow the regular behavior of the electromagnetic quantities.

This "hole" is necessary in order to get rid of the spurious divergence in the total charge Q from Equation (4.10). The expectation is that the value of x can be taken as small as possible, in order to vanish $x \to 0^+$ after all calculations were performed.

The material medium is then divided into 3 disjoint domains:

$$\text{Region1} : 0 < r < x;$$

$$\text{Region2} : x < r < R;$$

$$\text{Region3} : r > R.$$

Figure 4.1 gives a schematic idea of the proposed profile for the material medium.

The electric permittivity ϵ and the volumetric density of electric charge ρ for all the 3

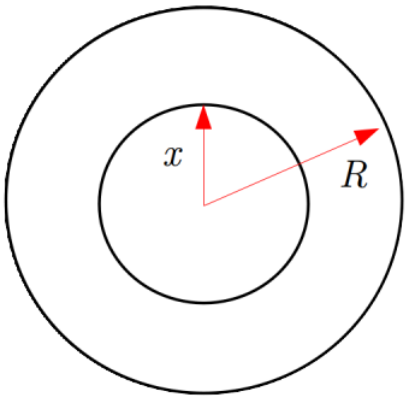

Figure 4.1: Profile of the proposed medium as a slab of area $4\pi r^2$ surrounded by vacuum, with an internal "hole" of area $4\pi x^2$. Material medium was divided in 3 regions: Region 1 ($r < x$), Region 2 ($x < r < R$), and Region 3 ($r > R$).

regions above have the general expressions

$$\epsilon = [\epsilon_1 - \epsilon_2]\,\Theta(x-r)\Theta(R-r) + [\epsilon_2 - \epsilon_3]\,\Theta(R-r) + \epsilon_3, \tag{4.11}$$

$$\rho = [\rho_1 - \rho_2]\,\Theta(x-r)\Theta(R-r) + [\rho_2 - \rho_3]\,\Theta(R-r) + \rho_3. \tag{4.12}$$

The electric permittivity ϵ_1 and the volumetric density of electric charges ρ_1 for Region 1 are, for simplicity, taken as constant quantities which agree with their corresponding inner limit from Region 2. Therefore, these quantities ϵ_1 and ρ_1 are evaluated from Region 2 as

$$\epsilon_1 = \epsilon_2|_{r\to x^+}, \tag{4.13}$$

$$\rho_1 = \rho_2|_{r\to x^+}. \tag{4.14}$$

Therefore, the parameters in Equations (4.11) and (4.12) are given by

$$\text{Region 1}\begin{cases} \epsilon_1 = \epsilon_0\left[\left(\dfrac{R}{x}\right)^{1+\beta} - 1\right]^{1-2\beta}, & 0 < r < x; \\ \rho_1 = \dfrac{\epsilon_0 E_0 x^{3\beta-2}}{(3\pi)^{\beta} R^{3\beta-1}}\left\{1 + \beta\left[\dfrac{7R^2(R^2-x^2)}{(R^2-2x^2)^2} - 1\right]\right\}, & 0 < r < x; \end{cases} \tag{4.15}$$

$$\text{Region 2}\begin{cases} \epsilon_2 = \epsilon_0\left[\left(\dfrac{R}{r}\right)^{1+\beta} - 1\right]^{1-2\beta}, & x < r < R; \\ \rho_2 = \dfrac{\epsilon_0 E_0 r^{3\beta-2}}{(3\pi)^\beta R^{3\beta-1}}\left\{1+\beta\left[\dfrac{7R^2(R^2-r^2)}{(R^2-2r^2)^2} - 1\right]\right\}, & x < r < R; \end{cases} \tag{4.16}$$

$$\text{Region 3}\begin{cases} \epsilon_3 = \epsilon_0\left[1 - \left(\dfrac{R}{r}\right)^{1+\beta}\right]^{1-2\beta}, & r > R; \\ \rho_3 = \dfrac{\epsilon_0 E_0 r^{3\beta-2}}{(3\pi)^\beta R^{3\beta-1}}, & r > R. \end{cases} \tag{4.17}$$

Note that Equations (4.11) and (4.12) hold almost everywhere but at $r = x$ and $r = R$; that is, the model constructed in this work does not provide the accurate mathematical expressions at the interfaces of these three regions.

4.2 Results from the parametrization

The numerical behavior of the parametrized physical quantities built in the previous Section 4.1 provides a consistent unification of the two analogue models carried out in Chapter 3.

4.2.1 The volumetric density of electric charge

The volumetric density of electric charge ρ is given by Equation (4.8), and it depends on the radial coordinate r and on the parameter β. Such representation is shown in Figure 4.2. The volumetric density of electric charge is constant throughout Region 1 (that is, for $r < x$). For this reason, the plot of ρ_1 is not shown in Figure 4.2. The figure displays the parametrized behavior of the volumetric density of electric charge in Regions 2 and 3 (that is, for $x < r < R$ and $r > R$ respectively).

For Region 2, two distinct behavior for the volumetric density of charge ρ occur: it may have either positive or negative values, depending on the value of the parameter β.

An abrupt step of the volumetric density of electric charge occurs at the interface between Regions 2 and 3 . This "leap" decreases in magnitude for large values of the parameter β, while for small values of it the step is amplified.

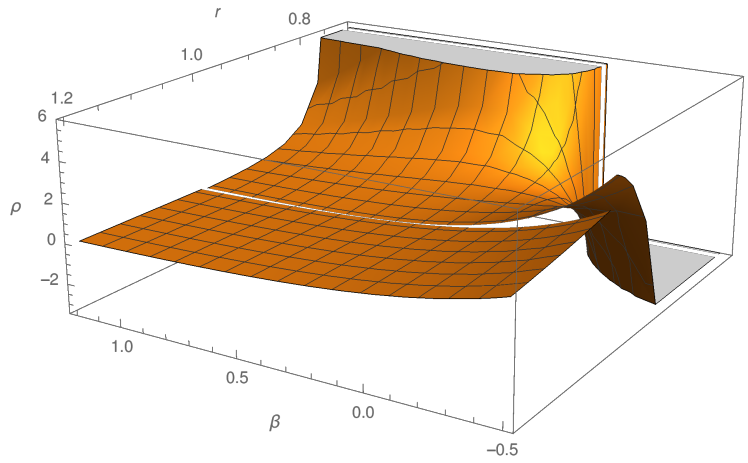

Figure 4.2: The parametrized volumetric density ρ of electric charge, with the choice $R = 1$ and $x = 1/\sqrt{2}$, where this latter arises from Equation (4.18) below.

4.2.2 The total electric charge

Formal integration of Equation (4.10) was calculated in the `Mathematica`$^{\text{TM}®©}$ platform, and the mathematical convergence requires an artificial restriction on the possible values of x and R. Such restriction is

$$x = R/\sqrt{2}. \tag{4.18}$$

The total electric charge contained inside a sphere of area $4\pi r^2$ is then obtained as the result of this integral. The numerical behavior of the total electric charge can be represented as a surface with parameters r and β, as shown in Figure 4.3.

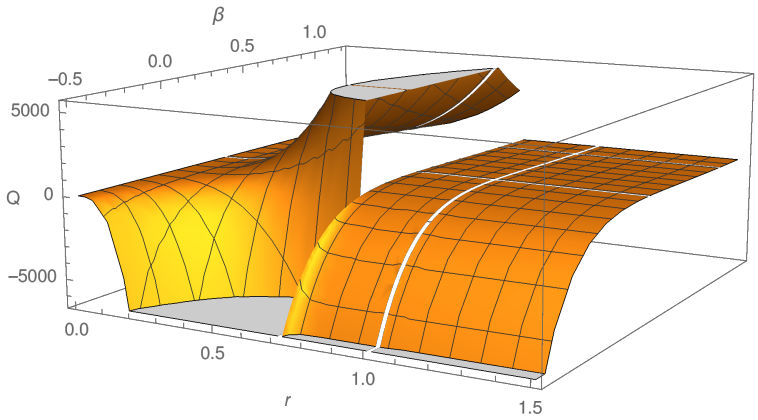

Figure 4.3: The amount of electric charge contained inside a sphere of area $4\pi r^2$ calculated by Equation (4.10), which the same choice $R = 1$ and $x = 1/\sqrt{2}$ for the parameters as in the previous diagram.

The most interesting behavior of this plot is the algebraic sign of the total electric charge, since there are regions with positive values, and regions with negative values for it. Abrupt changes of behavior for the total electric charge occur for both $r = x$ and $r = R$, precisely at the interfaces between these three regions. Note that the restriction imposed by integration in Equation (4.10) is clearly displayed in the plot: at $r = 1/\sqrt{2}$, there exists a "divergence" of the total electric charge.

4.2.3 The electric permittivity

The parametrized electric permittivity from Equation (4.4) is graphically presented in Figure 4.4.

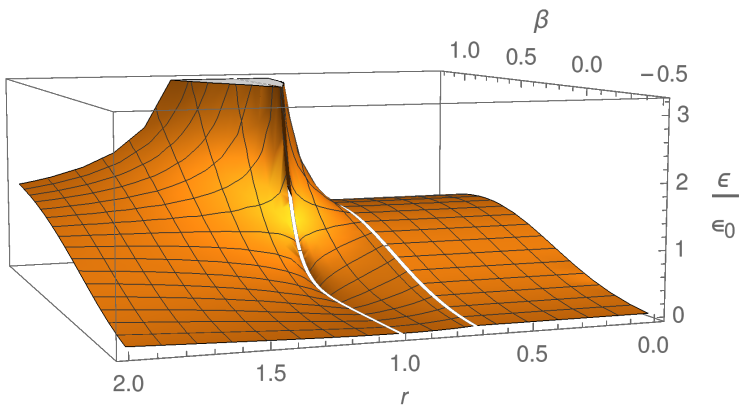

Figure 4.4: The normalized electric permittivity ϵ/ϵ_0, with the same choice $R = 1$ and $x = 1/\sqrt{2}$ for the parameters as adopted in the two previous diagrams. Assuming a fixed value for the parameter β, then ϵ/ϵ_0 is obviously a constant in Region 1, as shown in the plot. The lack of data at $r = R$ and $r = x$ is graphically interpreted as deprived of physical meaning.

The ratio ϵ/ϵ_0 have a very interesting behavior in these three regions. As show in Figure 4.4, there exists a smooth (or nearly smooth, at least) transition on the ratio ϵ/ϵ_0 for some special values of β: $\epsilon/\epsilon_0 > 1$ holds for $\beta > 1/2$, while $\epsilon/\epsilon_0 < 1$ holds for $\beta < 1/2$.

The electric permittivity from Equation (4.4), as shown in Figure 4.4, deserves to be analyzed separately in Region 1. For this Region, the electric permittivity is given by Equation (4.4) in the limit $r \to x^+$. With the substitution of x from Equation (4.18), it follows

$$\epsilon = \epsilon_0 \left(2^{\frac{1+\beta}{2}} - 1\right)^{1-2\beta}. \tag{4.19}$$

Figure 4.5 depicts Equation (4.19).

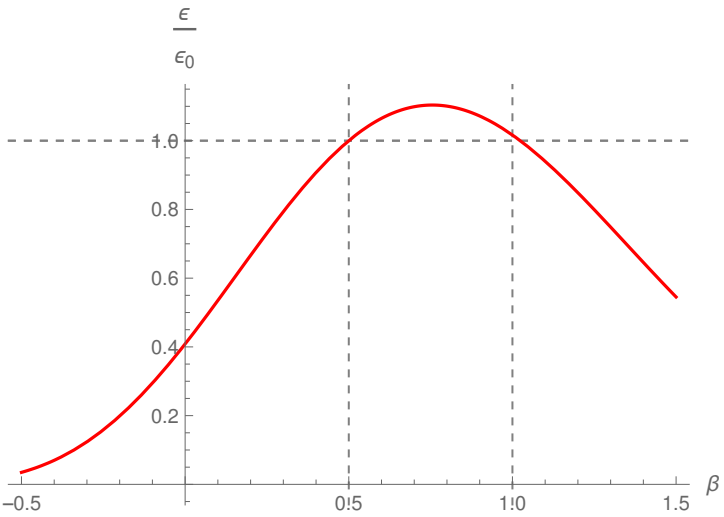

Figure 4.5: Electric permittivity ratio ϵ/ϵ_0 as function of the parameter β for Region 1 ($r < x$). Dashed lines were included for the sake of easy visualization of the distinguished value 1 of this quantity.

In Region 1, ϵ is constant for each value of β. In general, for conventional materials found in nature, such as common glass, one has $\epsilon > \epsilon_0$. This behavior is represented appropriately in Figure 4.5 for the range $1/2 < \beta < 1$. However, for values of β that are outside from this range (namely, for either $\beta > 1$ or $\beta < 1/2$), the peculiar $\epsilon < \epsilon_0$ behavior occurs. Materials that exhibit electric permittivity with values lower than the vacuum one are not found in nature. Thus, such materials must be manufactured in the laboratory, and today are better known as metamaterials. For both $\beta = 1/2$ and $\beta = 1$ cases, it follows $\epsilon = \epsilon_0$ exactly, as shown in Figure 4.5 explicitly.

In Region 2 ($x < r < R$), the electric permittivity varies from point to point according to the radial coordinate r, a given by Equation (4.17). The numerical behavior of the electric permittivity ϵ is most interesting at the Region 2. The electric permittivity given from Equation (4.17) is then plotted as a function of r and β in Figure 4.6, which displays an interesting behavior. Note that, for small values of the parameter β, the behavior of the ratio ϵ/ϵ_0 is independent of the radial coordinate, that is

$$\lim_{\beta \to -\infty} \epsilon/\epsilon_0 = 0. \tag{4.20}$$

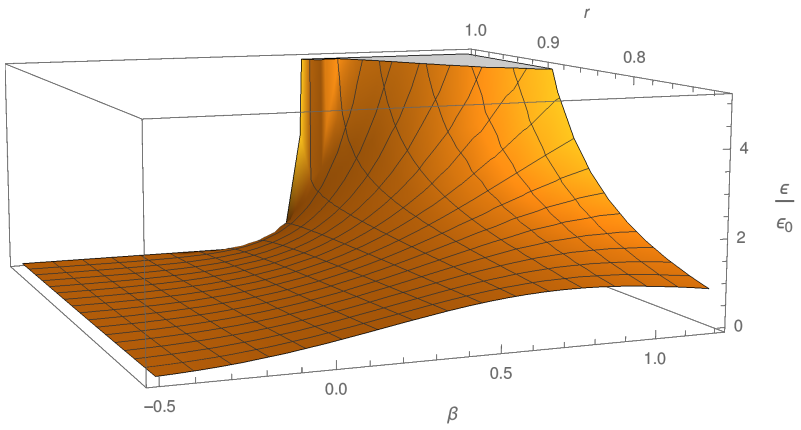

Figure 4.6: Electric permittivity ratio ϵ/ϵ_0 as a function of r and β for the Region 2 ($x < r < R$). For any fixed value of β such that $\beta > 1/2$, the ratio ϵ/ϵ_0 presents two distinct behaviors according with the value of the coordinate r: $\epsilon/\epsilon_0 \gg 1$ for the limit $r \to +\infty$ and $\epsilon/\epsilon_0 \simeq 1$ for $r \to 0^+$.

However, for any given value of β, two qualitatively distinct behavior for the electric permittivity occur, according with r. For large values of the coordinate r, the material displays a finite magnitude of the electric displacement vector field $\vec{D}$, even in the absence of the external (applied) electric field $\vec{E}$. At the regions where the cordinate r assume small values, the material presents a fairly weak polarization, instead.

Chapter 5

Conclusions

In this work, the construction of two optical analogue models, based on two well-known gravitational models, was presented: the Schwarzschild black hole model and the Ellis type of the Morris-Thorne wormhole model. A parametrization of these two analogue models was introduced, in order to obtain a class of (possibly analogue) models in terms of an arbitrary real parameter β. For each specific value of β, one has a different physical candidate of an analogue model. Note that the models for $\beta = 0$ and $\beta = 1$ are already known. However, the models for the other values of β are not known yet.

Mathematical convergence considerations (of the integral which evaluates the electric charge from Gauss law) require a finite size "hole" at the center of the sample. For simplicity, throughout this internal hole region, both the electric permitivity and the volumetric density of electric charge were taken as constants.

This work sought to quantify the difference between a black hole and a wormhole. These differences can be obtained by analyzing the behavior of analogue quantities according to the variation of the parameter β. The wormhole model is provided as the $\beta = 1$ case and, according with the plot of the electric permittivity, $\epsilon/\epsilon_0 > 1$. For $\beta = 0$, the black hole model is reproduced, and for this model $\epsilon/\epsilon_0 < 1$. Analyzing the plot of the electric permittivity in Figures 4.4, 4.5 and 4.6, it is apparent that $\epsilon/\epsilon_0 > 1$ for $\beta > 1/2$, and $\epsilon/\epsilon_0 < 1$ for $\beta < 1/2$. Therefore, the value of $\beta = 1/2$ is proposed as responsible for the interface between the two analogue structures, and provides the quantitative distinction between an analogue black hole and an analogue wormhole.

This work aimed to construct a parametrization which unifies an analogue model of a Schwarzschild black hole and as analogue model for the Ellis type of a Morris-Thorne wormhole. With such parametrization at hand, it is possible to investigate a new class of models that are different from those obtained for the values $\beta = 0$ and $\beta = 1$. For other values, it is not yet known which structure are being dealt with, thus opening possibilities for future studies.

Bibliography

[1] W. Gordon, "Zur lichtfortpflanzung nach der relativitätstheorie", Annalen der Physik **377**, 421 (1923).

[2] F. de Felice, "On the Gravitational field acting as an optical medium", Gen. Rel. Grav. **2**, 347 (1971).

[3] J. Plebanski, "Electromagnetic waves in gravitational fields", Phys. Rev. **118**, 1396 (1960).

[4] C. Barceló, S. Liberati, and M. Visser, "Analogue gravity", Living Reviews in Relativity **8**, 3 (2005).

[5] W. G. Unruh, "Experimental black-hole evaporation?", Phys. Rev. Lett. **46**, 1351 (1981).

[6] F. Belgiorno, S. L. Cacciatori, M. Clerici, V. Gorini, G. Ortenzi, L. Rizzi, E. Rubino, V. G. Sala, and D. Faccio, "Hawking radiation from ultrashort laser pulse filaments", Phys. Rev. Lett. **105**, 203901 (2010).

[7] S. Weinfurtner, E. W. Tedford, M. C. J. Penrice, W. G. Unruh, and G. A. Lawrence, "Measurement of stimulated hawking emission in an analogue system", Phys. Rev. Lett. **106**, 021302 (2011).

[8] K. Schwarzschild, "On the gravitational field of a mass point according to Einstein's theory", Sitzungsber. Preuss. Akad. Wiss. Berlin (Math. Phys.), 189 (1916).

[9] J. Foster and J. D. Nightingale, *A short course in general relativity* (Springer, New York, USA, 2006).

[10] R. D'inverno, *Introducing einstein's relativity* (Oxford University Press, New York, USA, 1992).

[11] M. S. Morris and K. S. Thorne, "Wormholes in spacetime and their use for interstellar travel: a tool for teaching general relativity", American Journal of Physics **56**, 395 (1988).

[12] R. Konoplya, "How to tell the shape of a wormhole by its quasinormal modes", Physics Letters B **784**, 43 (2018).

[13] E. B. Fonseca, *Eletrodinâmica não linear* (Private communication, 2018).

[14] E. Bittencourt, V. A. De Lorenci, R. Klippert, M. Novello, and J. M. Salim, "Analogue black holes for light rays in static dielectrics", Classical and Quantum Gravity **31**, 145007 (2014).

[15] D. J. Griffiths, *Introduction to electrodynamics* (Pretince Hall, New Jersey, USA, 1999).

[16] M. Novello and E. Goulart, *Eletrodinâmica não linear: causalidade e efeitos cosmológicos.* (Livraria da Física, São Paulo, 2010, In Portuguese).

[17] V. A. De Lorenci and G. P. Goulart, "Magnetoelectric birefringence revisited", Physical Review D **78**, 045015 (2008).

[18] J. Hadamard, *Leçons sur la propagation des ondes et les équations de l'hydrodynamique* (Paris: A. Hermann, 1903).

[19] A. Papapetrou, *Lectures on general relativity* (D. Reidel, Dordrecht, Holland, 1974).

[20] D. D. Pereira, *Estudo comparativo entre o formalismo eikonal e o formalismo das ondas de choque* (Universidade Federal de Itajubá, 2009, In Portuguese).

[21] R. L. Fernandez, *Propagação luminosa do espaço-tempo de Gödel* (Universidade Federal de Itajubá, 2016, In Portuguese).

[22] L. D. Landau and E. Lifshitz, *The classical theory of fields* (Pergamon Press Ltd, Oxford, 1975).

[23] M. Novello, S. P. Bergliaffa, J. Salim, V. A. D. Lorenci, and R. Klippert, "Analogue black holes in flowing dielectrics", Classical and Quantum Gravity **20**, 859 (2003).

[24] M. Novello and J. M. Salim, "Effective electromagnetic geometry", Phys. Rev. D **63**, 083511 (2001).

[25] H. G. Ellis, "Ether flow through a drainhole: a particle model in general relativity", Journal of Mathematical Physics **14**, 104 (1973).

[26] V. A. De Lorenci and R. Klippert, "Analogue gravity from electrodynamics in non-linear media", Physical Review D **65**, 064027 (2002).

[27] A. Riazuelo, "Seeing relativity-ii: revisiting and visualizing the reissner–nordström metric", International Journal of Modern Physics D **28**, 1950084 (2019).

[28] R. Adler, M. Bazin, and M. Schiffer, *Introduction to general relativity* (McGraw-Hill, New York, USA, 1975).

Appendix A

An analytic extension of Morris-Thorne analogue geometry

The Ellis model [25] for the Morris-Thorne solution [11], representing a wormhole, is given in standard (Gaussian spherical-like) coordinates as

$$g_{\mu\nu} = \mathrm{diag}\left[1, -\left(1-\frac{n^2}{r^2}\right)^{-1}, -r^2, -r^2\sin\theta\right], \tag{A.1}$$

which holds for $r > n$. Thus, such n is called the minimum 'radius' of the model. The corresponding invariant line element is

$$\mathrm{d}s^2 = \mathrm{d}t^2 - \mathrm{d}r^2\left(1-\frac{n^2}{r^2}\right)^{-1} - r^2\,\mathrm{d}\theta^2 - r^2\sin^2\theta\;\mathrm{d}\phi^2. \tag{A.2}$$

In order to extend such geometry for $r < n$, one follows similar procedure as the Kruskal-Szèckeres extension of Schwarzschild geometry (see the literature [28]) Thus, angular coordinates θ, ϕ are preserved, but time-like and "radial" coordinates should be respectively replaced by partially conformal coordinates v, u, as

$$\hat{\mathrm{d}s}^2 = [f(u,v)]^2\,(\mathrm{d}v^2 - \mathrm{d}u^2) - r^2(\mathrm{d}\theta^2 + \sin^2\theta\;\mathrm{d}\phi^2). \tag{A.3}$$

Comparison between the two metrics, that are in different coordinate systems, is given by the tensorial law

$$g_{\mu\nu} = \frac{\partial \hat{x}^{\alpha}}{\partial x^{\mu}} \frac{\partial \hat{x}^{\beta}}{\partial x^{\nu}} \hat{g}_{\alpha\beta}. \tag{A.4}$$

The 0-0, 1-1 and 0-1 components of Equation (A.4) are, respectively

$$f^2 \left[\left(\frac{\partial v}{\partial x^0} \right)^2 - \left(\frac{\partial u}{\partial x^0} \right)^2 \right] = 1, \tag{A.5}$$

$$f^2 \left[\left(\frac{\partial v}{\partial x^1} \right)^2 - \left(\frac{\partial u}{\partial x^1} \right)^2 \right] = - \left(1 - \frac{n^2}{r^2} \right)^{-1}, \tag{A.6}$$

$$\frac{\partial v}{\partial x^0} \frac{\partial v}{\partial x^1} = \frac{\partial u}{\partial x^0} \frac{\partial u}{\partial x^1}. \tag{A.7}$$

Another change of variables of the form

$$F(\xi) = \frac{1}{f^2(r)}, \tag{A.8}$$

in the previous equations yields

$$\left(\frac{\mathrm{d}\xi}{\mathrm{d}r} \right)^2 = \left(1 - \frac{n^2}{r^2} \right)^{-1}, \tag{A.9}$$

or, equivalently,

$$\frac{\mathrm{d}\xi}{\mathrm{d}r} = \pm \left(1 - \frac{n^2}{r^2} \right)^{-1/2}. \tag{A.10}$$

The solutions of the first-order ordinary differential Equation (A.10) give ξ as a function of the "radial" coordinate r in the form

$$\xi = \pm \sqrt{r^2 - n^2}. \tag{A.11}$$

Note that this solution is only valid for $r > n$.

For the range $0 < r < n$, the quantity ξ given by Equation (A.11) takes complex values, which is prohibited. Therefore, an improvement in the expression for ξ'^2 is required. Thus,

for the proposed 'internal' region, one has

$$\left(\frac{\mathrm{d}\xi}{\mathrm{d}r}\right)^2 = \left(\frac{n^2}{r^2} - 1\right)^{-1}, \tag{A.12}$$

the solution of which is

$$\xi = \mp\sqrt{n^2 - r^2}. \tag{A.13}$$

Note that the algebraic signs in Equations (A.11) and (A.13) are opposite to one another. The two solutions, external represented by Equation (A.11) and internal represented by Equation (A.13) can be graphically represented as shown in Figure A.1.

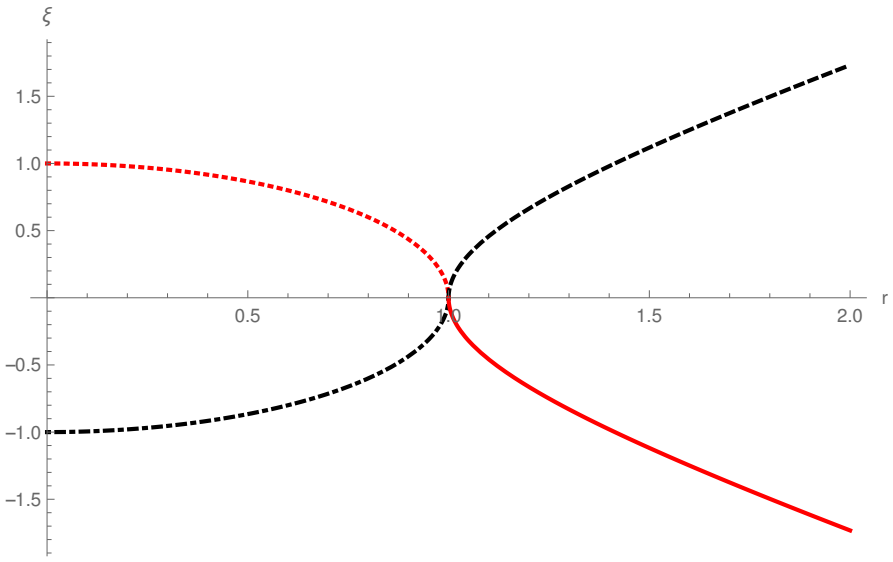

Figure A.1: The standard analytic extension of the Ellis model of Morris-Thorne geometry is depicted in both solid and dashed curves. The maximally extended manifold being proposed, which includes Ellis-Morris-Thorne solution in Equation (A.1) as a sub-manifold, is either the solid and dotted lines — the lower signs in Equations (A.11) and (A.13) — or the dashed and dot-dashed lines — the upper signs in Equations (A.11) and (A.13). — Lenght units are such that $n = 1$.

The proposed analytic extension intends to relate Equations (A.9) and (A.12). In this way, it becomes evident the need for the use of the absolute value function in the expression for ξ'^2

$$\left(\frac{\mathrm{d}\xi}{\mathrm{d}r}\right)^2 = \left|1 - \frac{n^2}{r^2}\right|^{-1}, \tag{A.14}$$

with solutions

$$\xi = \pm\sqrt{|r^2 - n^2|}\,\mathrm{sgn}(r - n). \tag{A.15}$$

The two algebraic signs in Equation (A.15) correspond to two alternatives for the analytic extension of Morris-Thorne geometry to the 'inner' region $r < n$: either the + sign (depicted in Figure A.1 as dashed and dot-dashed lines), or else the - sign (depicted as solid and dotted lines in Figure A.1). Thus, the analytic extension of Morris-Thorne proposed by Equation (A.15) induces in Equation (A.1) a modification in the "radial" component of the metric. Therefore, the here proposed maximal extension of Ellis type of Morris-Thorne metric is

$$g_{\mu\nu} = \text{diag}\left[1, -\left|1 - \frac{n^2}{r^2}\right|^{-1}, -r^2, -r^2\sin^2\theta\right]. \tag{A.16}$$

Appendix B

The Mathematica™®© code

This appendix B provides the algorithmic code used in the `Mathematica`™®© plataform which generates the plots shown in Chapter 4.

Electric permittivity

```
Plot3D[(((((1/0.71)^(1+β) - 1)^(1-2 β) - (((1/r)^(1+β) - 1)^(1-2 β)) HeavisideTheta[0.71 - r] HeavisideTheta[1 - r] +
 (((((1/r)^(1+β) - 1)^(1-2 β) - (1 - (1/r)^(1+β))^(1-2 β)) HeavisideTheta[1 - r] +
 (1 - (1/r)^(1+β))^(1-2 β), {β, -0.5, 1.2}, {r, 0, 2}]
```

Region 1 - Electric permittivity

```
(((n/x)^(1+β) - 1)^(1-2 β) /. {x → 0.71, n → 1}
```

$$(-1 + 1.40845^{1+\beta})^{1-2\beta}$$

```
Plot[(-1 + 1.4084507042253522`^(1+β))^(1-2 β),
 {β, -0.5, 1.5}, AxesLabel → Automatic, PlotStyle → Red]
```

Region 2 - Electric permittivity

```
((n/r)^(1+β) - 1)^(1-2 β) /. {n → 1}
```

$$\left(-1 + \left(\frac{1}{r}\right)^{1+\beta}\right)^{1-2\beta}$$

```
Plot3D[(-1 + (1/r)^(1+β))^(1-2 β), {β, -0.5, 1.2}, {r, 0.71, 1},
 AxesLabel → Automatic, BoundaryStyle → Thick, PlotStyle → Orange]
```

Volumetric density of electric charge

```
Plot3D[(0.72`^(-1+2 β) (3 π)^-β (1 + 2488.3667296786466` β) - r^(2 β-1)/((3 π)^β 1^(3 β-1)) (1 + β (7 * 1^2 (1^2 - r^2)/(1^2 - 2 r^2)^2 - 1))) HeavisideTheta[0.72 - r] × HeavisideTheta[1 - r] +
 (r^(2 β-1)/((3 π)^β 1^(3 β-1)) (1 + β (7 * 1^2 (1^2 - r^2)/(1^2 - 2 r^2)^2 - 1)) - r^(2 β-1)/((3 π)^β 1^(3 β-1))) HeavisideTheta[1 - r] +
 r^(2 β-1)/((3 π)^β 1^(3 β-1)), {β, -0.5, 1.2}, {r, 0.71, 1.2}]
```

Total electric charge

```
Plot3D[4 × 0.71`^(-2+3 β) × 3^(-1-β) π^(1-β) y^3 (1 + 51624.520523498104` β) * HeavisideTheta[0.71 - y] +
 (1 - HeavisideTheta[0.71 - y]) * 4 * π * (3 π)^-β (((0.71`^(3 β) y - 0.71` y^(3 β))/(0.71` y - 2.13` y β) -
 1.4084507042253522` (-0.71` + 0.71`^(3 β)) β (-1 + HeavisideTheta[1 - y])/(-1 + 3 β) -
 (0.71`^(3 β) y - 0.71` y^(3 β)) β HeavisideTheta[1 - y]/(0.71` y - 2.13` y β) -
 1/(-5 + 3 β) 591.4287837853212` e^(-3/2 i π β) β (1 - HeavisideTheta[1 - y])) (-1.0082` (-0.0029348701999999394` + 0.71`^(3 β)) (-5 + 3 β) - 0.004438404203459991`
 (-1 + β) HypergeometricPFQ[{1, 1/2 (5 - 3 β), 1/2 (7 - 3 β)}, {1/2}] + 0.024599999999999955` ×
```

$$0.71^{3\beta}(-1+\beta)\,\text{Hypergeometric2F1}\left[1,\frac{1}{2}(5-3\beta),\frac{1}{2}(7-3\beta),0.9918666931164452\right]\Bigg)$$

função 2F1 hipergeométrica

$$\left(\text{Cos}\left[\frac{3\pi\beta}{2}\right]+i\,\text{Sin}\left[\frac{3\pi\beta}{2}\right]\right)+\frac{1}{-1+\beta}\left(0.+99.3797499687268\,i\right)e^{-\frac{3}{2}i\pi\beta}\,\beta$$

cosseno seno

$$(1-\text{HeavisideTheta}[1-y])\Bigg(-3.0246\left(-0.005821999999999994+0.71^{3\beta}\right)(-1+\beta)-$$

função teta de Heaviside

$$0.0029348701999999944\,(-1+3\beta)\,\text{Hypergeometric2F1}\left[1,-\frac{3}{2}(-1+\beta),\frac{1}{2}(5-3\beta),\frac{1}{2}\right]+$$

função 2F1 hipergeométrica

$$0.008199999999999985\times 0.71^{3\beta}(-1+3\beta)$$

$$\text{Hypergeometric2F1}\left[1,-\frac{3}{2}(-1+\beta),\frac{1}{2}(5-3\beta),0.9918666931164452\right]\Bigg)$$

função 2F1 hipergeométrica

$$\left(-i\,\text{Cos}\left[\frac{3\pi\beta}{2}\right]+\text{Sin}\left[\frac{3\pi\beta}{2}\right]\right)+\frac{1}{5-3\beta}\,7\times 2^{-\frac{7}{2}+\frac{3\beta}{2}}\,e^{-\frac{1}{2}i(-1+3\beta)(\pi-i\,\text{Log}[2])}\,\beta$$

cosseno seno

$$\text{HeavisideTheta}[1-y]\Bigg(\left(0.-121.95121951219534\,i\right)0.71^{-5+3\beta}\,\text{Cos}\left[\frac{3\pi\beta}{2}\right]$$

função teta de Heaviside cosseno

$$\Bigg(1.0082\,(5-3\beta)+0.024599999999999955\,(-1+\beta)\,\text{Hypergeometric2F1}\left[1,\frac{1}{2}(5-3\beta),\right.$$

função 2F1 hipergeométrica

$$\left.\frac{1}{2}(7-3\beta),0.9918666931164452\right]\Bigg)+\frac{1}{-1+2y^2}i\,y^{-5+3\beta}\,\text{Cos}\left[\frac{3\pi\beta}{2}\right]\Bigg(2y^2(5-3\beta)+$$

cosseno

$$3\left(-1+2y^2\right)(-1+\beta)\,\text{Hypergeometric2F1}\left[1,\frac{1}{2}(5-3\beta),\frac{1}{2}(7-3\beta),\frac{1}{2y^2}\right]\Bigg)+$$

função 2F1 hipergeométrica

$$121.95121951219534\times 0.71^{-5+3\beta}\Bigg(1.0082\,(5-3\beta)+0.024599999999999955$$

$$(-1+\beta)\,\text{Hypergeometric2F1}\left[1,\ \frac{1}{2}(5-3\beta),\ \frac{1}{2}(7-3\beta),\ 0.9918666931164452`\right]\Bigg)$$

função 2F1 hipergeométrica

$$\text{Sin}\left[\frac{3\pi\beta}{2}\right]-\frac{1}{-1+2y^2}y^{-5+3\beta}\Bigg(2y^2(5-3\beta)+3\left(-1+2y^2\right)(-1+\beta)$$

seno

$$\text{Hypergeometric2F1}\left[1,\ \frac{1}{2}(5-3\beta),\ \frac{1}{2}(7-3\beta),\ \frac{1}{2y^2}\right]\Bigg)\text{Sin}\left[\frac{3\pi\beta}{2}\right]\Bigg)-$$

seno

$$\frac{1}{3(-1+\beta)}7\times 2^{\frac{1}{2}(-5+3\beta)}e^{-\frac{1}{2}i(1+3\beta)(\pi-i\,\text{Log}[2])}\beta\,\text{HeavisideTheta}[1-y]$$

função teta de Heaviside

$$\Bigg(\left(0.`-121.95121951219534`\,i\right)0.71`^{-3+3\beta}\,\text{Cos}\left[\frac{3\pi\beta}{2}\right]$$

cosseno

$$\Bigg(-3.0246`(-1+\beta)+0.008199999999999985`(-1+3\beta)$$

$$\text{Hypergeometric2F1}\left[1,\ -\frac{3}{2}(-1+\beta),\ \frac{1}{2}(5-3\beta),\ 0.9918666931164452`\right]\Bigg)+$$

função 2F1 hipergeométrica

$$\frac{1}{-1+2y^2}i\,y^{-3+3\beta}\,\text{Cos}\left[\frac{3\pi\beta}{2}\right]\Bigg(-6y^2(-1+\beta)+\left(-1+2y^2\right)(-1+3\beta)$$

cosseno

$$\text{Hypergeometric2F1}\left[1,\ -\frac{3}{2}(-1+\beta),\ \frac{1}{2}(5-3\beta),\ \frac{1}{2y^2}\right]\Bigg)+$$

função 2F1 hipergeométrica

$$121.95121951219534`\times 0.71`^{-3+3\beta}\Bigg(-3.0246`(-1+\beta)+0.008199999999999985`$$

$$(-1+3\beta)\,\text{Hypergeometric2F1}\left[1,\ -\frac{3}{2}(-1+\beta),\ \frac{1}{2}(5-3\beta),\ 0.9918666931164452`\right]\Bigg)$$

função 2F1 hipergeométrica

$$\text{Sin}\left[\frac{3\pi\beta}{2}\right]-\frac{1}{-1+2y^2}y^{-3+3\beta}\Bigg(-6y^2(-1+\beta)+\left(-1+2y^2\right)(-1+3\beta)\,\text{Hypergeometric2F1}\Big[$$

função 2F1 hipergeométrica

$$1, -\frac{3}{2}(-1+\beta), \frac{1}{2}(5-3\beta), \frac{1}{2y^2}\Big]\Big)\text{Sin}\Big[\frac{3\pi\beta}{2}\Big]\Big)\Big), \{y, 0, 1.5\}, \{\beta, -0.5, 1.2\}\Big]$$

seno